Impact assessment of coastal hazards due to typhoons in the Marshall Islands

Kees Nederhoff[1], Alessio Giardino[1]

[1] Deltares, Unit Marine and Coastal Systems, The Netherlands

Keywords:

1. Abstract

Climate change and sea level rise are a global threat to coastal areas and, in particular, to small island states. Future projections indicate that sea levels are expected to rise in the next century at different rates in multiple regions around the world. On top of that, the intensity and frequency of extreme events such as typhoons may vary. In this study, the impacts in terms of flooding of different typhoon conditions are assessed in the present day conditions as well as accounting for climate change effects. In particular, the assessment is carried out for the island of Ebeye, located on Kwajalein Atoll (Republic of Marshall Islands).

The results presented herein show that coastal engineering experiences at traditional coasts cannot be applied one-on-one to small islands states in the Pacific, because the relevant hydrodynamic processes offshore and on the reef are fundamentally different. These processes can be examined using a modeling approach combining parametric wind models, as well as process-based models such as Delft3D and XBeach. The model results suggest that offshore extreme wave and storm surge levels may increase by up to 6-8% as a result of higher typhoon winds. Nevertheless, the projected sea level rise is by far the dominant process in relation to increase in flooding levels, accounting for about 80% of the total increase in flooding impacts.

2. Introduction

Typhoons are among some of the nature's most powerful and destructive phenomena. However, extensive datasets on the impacts of typhoons are absent for most developing countries and small island states. Nevertheless, numerical simulations can be used to identify the coastal hazards (i.e. wave heights and oceanic water levels) and impacts (i.e. flooding) resulting from the high wind speeds and large pressure drops of typhoons and tropical storms.

Another advantage of numerical simulations is that scenarios simulations can be carried out, in order to improve the risk assessments, spatial planning and disaster risk reduction measures of the impacted areas. Additionally, assessments can be carried out for current and future scenarios as a result of climate change. Within the scientific community, there is a general consensus that oceanic water levels will increase in the future (IPCC, 2013). However, it is less clear how typhoons and tropical storms may change as a result of climate change (Knutson et al., 2010).

Walsch et al. (2012) reviewed the current understanding of the effect of climate change on extreme sea levels in the Pacific region. Large uncertainties remain in the exact projections of the regional variations in sea level rise (Church et al., 2010). However, the overall trend of increasing oceanic water levels in the Pacific are clear. For the projected intensification of typhoons (i.e. both larger pressure drops or higher wind speeds) there is more scatter (either more or less intense typhoons). However, Walsch et al. (2012) concluded that, generally, finer resolution model simulations (e.g. Hasegawa & Emori, 2005 and Knutson et al., 2010) suggested that the most intense typhoons are likely to become more intense.

An important component of typhoon modeling relates to the estimation of the wind field used as an input parameter for the modeling. Parametric radial profiles of typhoon winds form the basis of the current approaches, since often detailed wind fields based on observations are not available. Fujita (1952) developed one of the first radial wind models to estimate surface wind and pressure fields (two-dimensional information) during typhoons. In engineering applications, the Holland profile (Holland, 1980 and Holland et al, 2010) is often used. Major input parameters of this relationship are: the location of the eye of the typhoon and a quantification of the maximum sustained wind speed derived from best-track data from meteorological agencies.

Since the information in historical databases is often not sufficient to provide all the necessary input parameters of a wind model, additional parametric relationships have been developed to estimate the necessary inputs of the wind profile. For example, in order to describe the internal winds, the radius of maximum winds (RMW) is needed but is only reported by meteorological agencies after the 1980s. To estimate the RMW, several relationships exist (e.g. Gross et al., 2004, Vickery and Wadhera, 2008). However, these relations are often only derived for the Atlantic and/or Eastern Pacific and are therefore not necessarily correct for other oceanic basins. Nederhoff et al. (in preparation) derived consistent relationships for all oceanic basins including the Central and Western Pacific, for both the RMW and gale force winds (average difference in radius of 35 knots; ∆AR35). Those relationships result in better (mean) forecasts, in terms of coastal hazards resulting from wave height and storm surge level, than the relationships available from literature.

The hydrodynamic conditions on coral reefs are inherently different compared to coastlines with shallow or wide continental shelf. Wave breaking along the reef results in an increase of the water level due to wave-induced setup (Gerritsen, 1980; Vetter et al., 2010). Moreover, infragravity waves are generated in the 25–1000s band (Symonds et al., 1982; Pomeroy et al., 2012; Gawehn et al., 2016). These processes can lead to large wave runup and flooding of the atoll and are therefore important to take into account when considering impacts of coastal hazards on atolls. Quataert et al. (2015) showed that the XBeach-surfbeat model (Roelvink et al., 2009) can be used to accurately simulate wave runup and flooding at atoll islands.

In this study, the state-of-the-art hydrodynamic and wave model Delft3D-FLOW (Lesser et al., 2004) and Delft3D-WAVE (SWAN) (Booij, et al., 1999) forced with parametric wind and pressure fields, are used to simulate respectively oceanic water levels and waves as a result of typhoons. The numerical model XBeach-surfbeat is used to translate the deep water hazards into nearshore impacts (atoll flooding) on the island of Ebeye (The Republic of the Marshall Islands, RMI). The generic multi-hazard and risk assessment methodology is described in Giardino et al. (in preparation).

The goal of this paper is to assess the effect of sea level rise and/or the potential increase in typhoons wind speeds on atoll flooding for the coral reef island of Ebeye. Section 3 elaborates further on the material and methods supporting the paper. The results are described in Section 4 and discussed in Section 5. Finally, Section 6 summarizes the main conclusion from the study.

3. **Materials and method**

General approach

The methodology proposed to assess impacts of coastal hazards due to typhoons on Ebeye Island is based on a modeling train including the following models (see Figure 1):

1. **Atmospheric hazards** (wind and pressure) are described by the typhoon wind profile. The approach of Nederhoff et al. (in preparation) is followed, which applies the Holland et al. (2010) wind model in combination with additional formulations to describe the RMW and gale force winds and takes into account typhoon asymmetry according to Schwerdt et al. (1979).
2. **Deep water coastal hazards** (waves and ocean water levels) are simulated by means of a coupled Delft3D-FLOW and Delft3D-WAVE (SWAN) simulation. Delft3D-FLOW resolves the depth-averaged, nonlinear shallow water (NLSW) equations that result from tidal and meteorological forcing. SWAN is a third-generation shallow water wave model, which solves the discrete spectral action balance equation. The model accounts for the effects of wind growth, wave dissipation due to whitecapping, bottom friction, wave breaking, non-linear wave-wave interactions, wave refraction, and shoaling.
3. **Nearshore impact** (atoll flooding) is simulated with the XBeach-surfbeat model. XBeach-surfbeat resolves water level variations up to the scale of long (infragravity) waves using the depth-averaged, NLSW equations and consists of formulations for short wave envelope propagation (time-dependent wave action balance).

Coastal hazards and impact as a result of typhoons are assessed for different return periods (T = 5, 10, 30, 50 and 100 years) by means of an extreme value analysis (EVA) based on the Delft3D model results for the individual typhoon tracks. XBeach model simulations were only carried out for the selected return periods in combination with the derived extreme values for waves and water levels. Moreover, simulations were carried out for different future scenarios to account for the effect of climate change. In particular, the relative effect of sea level rise and increase in typhoon wind speeds have both been assessed and compared.

Figure 1 Flow chart of the proposed methodology to assess the impacts at Ebeye Island

Site description

The area of interest is located in the Pacific Ocean. The Republic of the Marshall Islands (left panel of Figure 2) consists of 29 atolls and 5 reef platforms arranged in a double chain of islands named Ratik and Ralik (Owen at al., 2016). The atolls and reef platforms are host to approximately 1,225 reef islands, which are characterized as low-lying with a mean elevation of 2 m above mean sea level (MSL). Many of the islands are inhabited, with over 74% of the 53,000 inhabitants (2011 census) concentrated on the atolls of Majuro and Ebeye. The focus of this study is on the island of Ebeye.

Ebeye is built on a small reef on the south-eastern side of Kwajalein Atoll (8.78°N 167.74°E), (right panel of Figure 2). The island stretches for about 2 km from north to south and it is approximately 250 m wide. The island borders a large lagoon to the west and the open ocean to the east. The lagoon is shallow with an average depth of approximately 40 m. On the eastern ocean side, the islet is fronted by a reef flat. This reef flat varies slightly in width between 100-130 m. From there on, the depth quickly increases, reaching depths of ~6000 m just a few kilometers out the coast. The islet is covered entirely with buildings and infrastructure and is densely populated with 12,000 inhabitants.

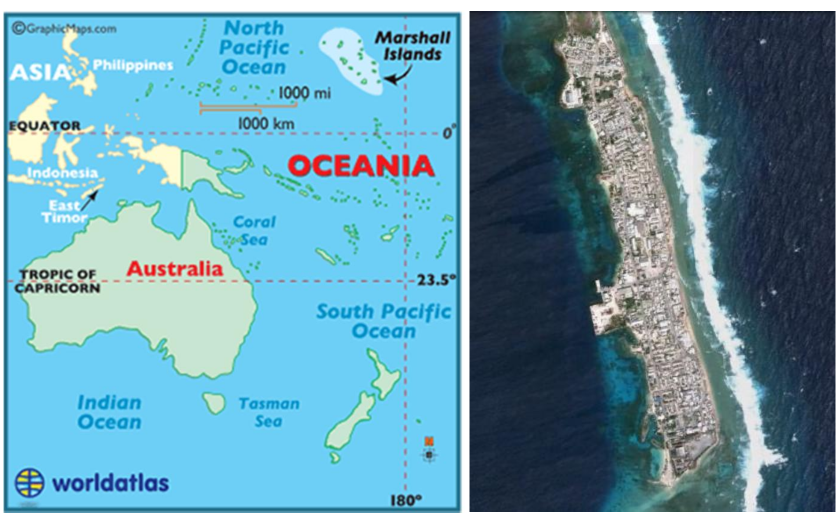

Figure 2 Geographical location of the Republic of the Marshall Islands (left panel) (source: http://www.worldatlas.com/webimage/countrys/oceania/mh.htm). Aerial view of the island of Ebeye (right panel)

Data

Bathymetry

Deep water bathymetry was derived as a combination between bathymetric data of the Republic of the Marshall Islands and Vicinity (Hein et al., 2007) and GEBCO (General Bathymetric Charts of the Ocean, http://www.gebco.net/) global bathymetric data sets. Hein et al. (2007) compiled the data set from surveys conducted by the USGS, Korean Ocean Research and Development Institute (http://pubs.usgs.gov/mf/1999/2324). The GEBCO's gridded bathymetric data sets are global terrain models for ocean and land and include the GEBCO_2014 Grid, which is a global 30 arc-second interval grid of 1 by 1 km.

For the quantification of the effects of coastal hazards on the island, detailed bathymetric measurements in the intertidal area are required since these areas are not included in the above datasets. These data were collected during a field mission (Giardino et al., 2016) by means of an echo sounder (Plastimo echotest: resolution 0.1 m – maximal measurable depth = 80 m) on a number of cross-shore transects from the shore down to a depth of 80 m.

Topography

Detailed topographic data are essential for carrying out an impacts assessment on low-lying atoll islands such as Ebeye. This data was derived during a survey of the island of Ebeye including all the coastal defenses (Giardino et al., 2016). Measurements were collected by means of a Trimble CenterPoint-RTX with a maximum vertical accuracy of 10 cm. The data collected were first corrected based on field observations and then interpolated in order to create a digital elevation map (DEM) of the island. It is worth noting that both topographic and bathymetric surveys were carried out with a relatively simple instrument due to severe time/budget limitations.

Water levels

Extreme total oceanic water levels are the result of the contributions from the MSL, the tide and the combined effect of pressure drop, wave induced set-up and wind-driven surge. Time series of tidal elevation were obtained from the TOPEX/POSEIDON Global Inverse Solution (Egbert and Erofeeva, 2002). In particular, 10-year tidal data were analyzed to obtain the maximum water level due to tidal effects. The contributions due to typhoons (deep water surge) was simulated with a Delft3D model for deep water coastal hazards (Section 4).

As a result of climate change, the mean sea level is expected to increase. The various scenarios of sea level rise are illustrated in Representative Concentration Pathways (RCPs). Table 1 describes different sea level rise scenarios for the years 2030, 2050, and 2100 (CSIRO, 2014) for Pacific islands. In this paper, a conservative (i.e. worst-case scenario) estimate of sea level rise in 2100 of 0.78 m was used.

Table 1 Sea level rise for different time horizons and RCP scenarios (CSIRO, 2014).

RCP scenario	2030	2050	2100
4.5	0,12	0,23	0,53
8.5	0,13	0,26	0,78

Typhoon tracks

The IBTrACS database (International Best Track Archive for Climate Stewardship; https://www.ncdc.noaa.gov/ibtracs/) is the most complete global set of historical typhoons available and describes the location, wind speed and pressure drop of the typhoon every six-hours (Figure 3). In Table 5 the full list of typhoons for the period 1950-2013 which have hit the RMI with wind speeds of more than 18 m/s is reported.

Based on the IBTrACKS data, it is concluded that storm systems around the RMI have a median wind speed of 23.6 m/s with a median pressure of 987 mbar. In fact, the majority of rapidly rotating storm systems at RMI is lower than the typhoon category, as defined by the Saffir-Simpson scale (i.e. tropical depressions or tropical storms). The 1% exceeded wind speed and pressure in the area are 68.7 m/s (category 4) and 888 mbar.

Future projections based on Knutson et al. (2010) indicate that greenhouse warming will result in a decrease in the number of typhoons. However, the forecasted globally averaged intensity of typhoons will increase by 2–11% by 2100. In this paper, a conservative (i.e. worst-case scenario) estimate of increase in intensity (wind speed and pressure drop) by 11% is used. This is in line with Hasegawa & Emori (2005) who estimated the intensification of typhoons in the West Pacific at 8.4%.

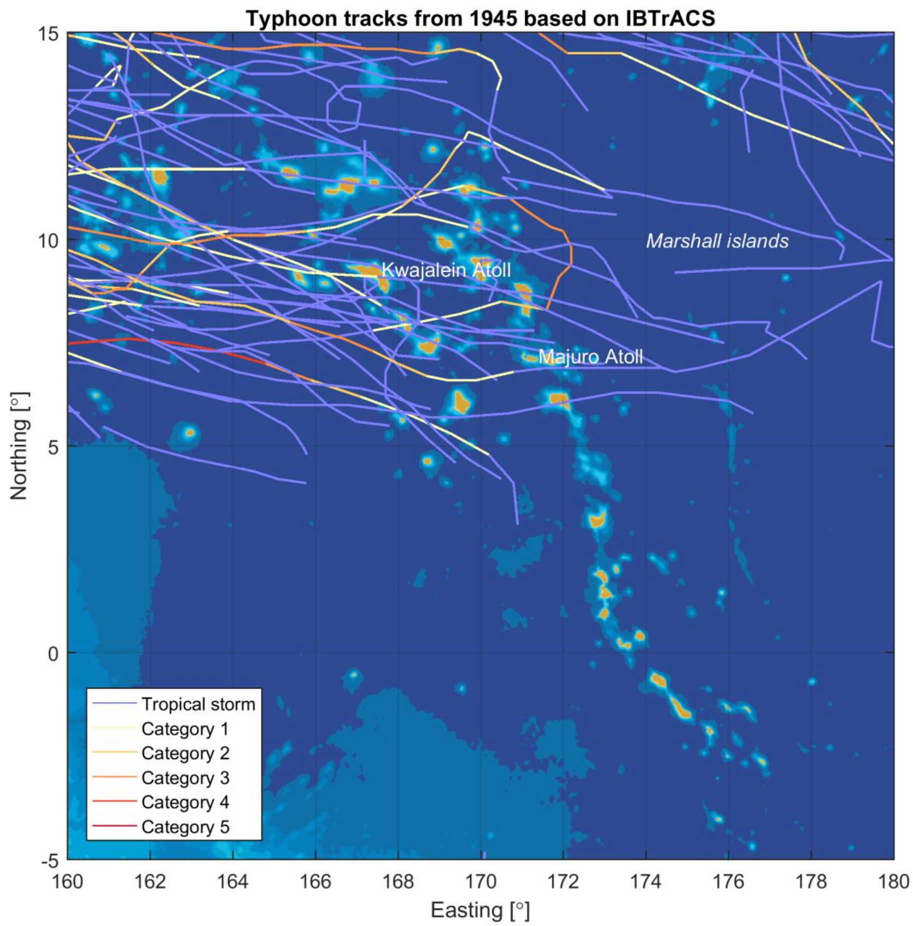

Figure 3 Typhoon tracks from 1950 across the study area per category based on IBTrACS database (https://www.ncdc.noaa.gov/ibtracs/. Colours indicate Saffir-Simpson scale).

Model setup

Wave and surge model: Delft3D FLOW and WAVE

In order to determine the surge and significant wave height near Ebeye as a result of typhoons, a Delft3D-FLOW and WAVE model of the area of interest (Northing: -5 till 15 degrees, Easting: 160 till 180 degrees) was set-up (Figure 4). The model contains 200 x 200 grid cells. These models are used to describe the deep water conditions, providing the boundary conditions to an XBeach model set-up to propagate offshore conditions to nearshore and determine the impact (i.e. flooding) at Ebeye.

The only forcing in the model are the wind speeds and pressure drops from the selected typhoons. This means that all waves are generated inside the model domain as no additional boundary conditions are imposed. Additionally, water level variations due to meteorological forcing consist of the residual water level (i.e. surge), since no tidal water level variations from the boundaries or inside the model are used. All the typhoon conditions simulated are summarized in Table 5. The table describes the maximum sustained wind speed and minimal pressure drop for each typhoon condition. However, in the IBTrACKS database, additional information is provided and related to the track position and matching wind speed and/or pressure drop. This information, in combination with the additional parametric relationships for the RMW and gale force winds based on Nederhoff et al. (in preparation), is needed to create a spatially and temporally varying wind and pressure for the entire time span of a storm.

Computational results for waves (i.e. wave height, period and direction) and water levels (i.e. surge) in the form of time series are extracted from the model near Ebeye. The time series are used to determine the maximum wave height (with matching peak wave period) that occurred during each typhoon and will form the basis of the extreme value analysis of the waves generated by the different typhoons. Furthermore, surge levels are determined in a similar matter.

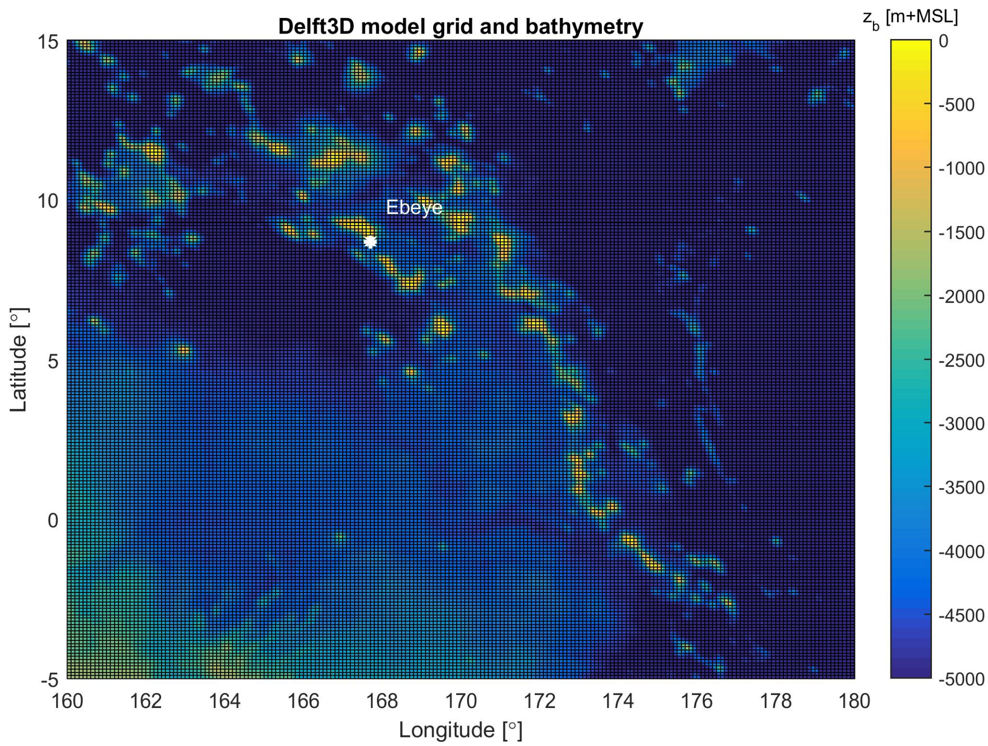

Figure 4 Delft3D model setup: applied grid and bathymetry for the typhoon modeling around the Marshall Islands. With the white star the observation points near Ebeye is shown.

Atoll flooding: XBeach

The deep water hazards are translated into nearshore impacts (i.e. atoll flooding) using a two-dimensional XBeach model of Ebeye. The model is used to simulate the atoll flooding as a result of wave and water level conditions for five different return periods (T = 5, 10, 30, 50 and 100 years). The modeling study will result in two-dimensional maps of flooding depths over the island for different return periods.

The topography and grid resolution of the XBeach model are shown in Figure 5. The XBeach grid consists of 519x138 (cross-shore x longshore) grid cells. In longshore direction, the grid is equally spaced with a resolution of 20 m, it decreases from 20 m (offshore) to 1 m (nearshore) in cross-shore direction. The model is somewhat extended in longshore direction in order to overcome any lateral boundary effects.

The bed roughness is non-uniform with Chezy values ranging between 30 to 60 $m^{1/2}\ s^{-1}$. Offshore and on the reef flat, the bathymetry is assumed to be relatively smooth. The fore reef, on the other hand, is quite rough as large coral canopies are known to create a course relief in these parts. Furthermore, the island itself represents a rough surface for overtopping waves. At areas with higher bed roughness a lower Chezy coefficient is applied.

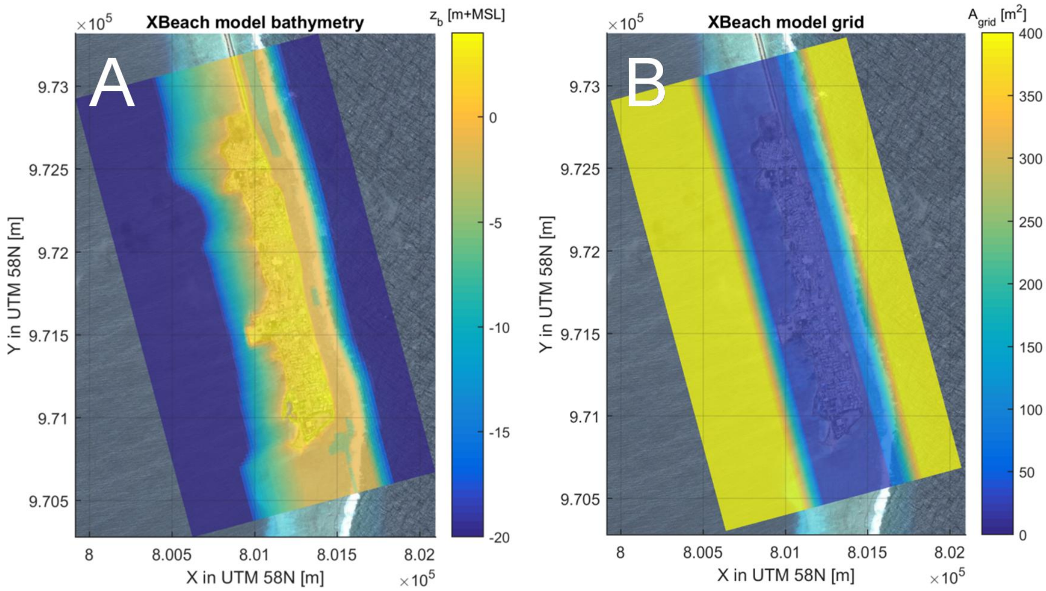

Figure 5 XBeach model set-up. Subfigure A) depicts the topography as implemented in the model. Subfigure B) shows the cell sizes in m^2.

Wave conditions from the ocean attack the coastline from the east in shore-normal direction. On the lateral boundaries, Neumann conditions are imposed. Typhoon scenarios are simulated assuming a design storm with duration of 30 hours with a time series of water levels and waves. This design storm includes approximately three tidal cycles with a spring-high tide during the peak of the storm, occuring 15 hours after the start of the simulation (Figure 6). Besides the periodical water level modulation by the tide, this also includes stationary storm surges and sea level rises which vary for different return periods and future scenarios. Given the small size of the domain, all water level changes that are imposed occur simultaneously across the entire model domain.

Prescribed deep water waves increase linearly from an initial arbitrary value of 1.5 m towards their maximum value at the peak of the design storm (i.e. after 15 hours). This maximum value depends on the specific return period. After this peak, the wave heights decrease again to 1.5 m towards the end of the simulation. The maximum wave height also depends on the return period and future scenarios and hence varies between simulations.

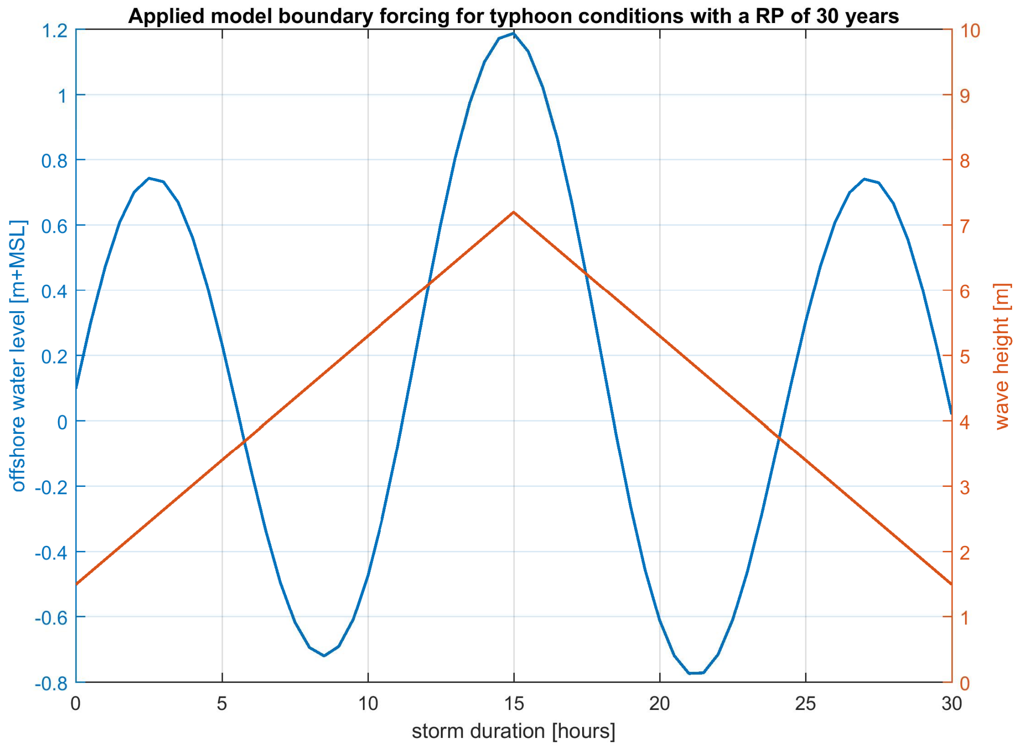

Figure 6 Applied time series of water levels and wave heights in XBeach for typhoon conditions with a return period of 1/30 years.

4. **Results**

Deep water coastal hazards: waves and storm surge levels

From each of the 47 typhoon simulations, the water level and waves are computed (Figure 7 and Figure 8). The maxima during each simulation have been stored, which will be used as input to the nearshore XBeach modeling. The result provides an overview of the maximum observed significant wave height and maximum storm surge level during the different simulated typhoons as can be seen in Figure 9 for the current scenario (blue) and the future scenario (yellow). In the future scenario it is assumed, based on Knutson et al. (2010), that typhoons will increase in intensity by 11% (both larger pressure drops and higher maximum sustained wind speeds).

Based on these results, one can see that a typhoon with higher sustained wind speeds does not necessarily result in higher wave heights at Ebeye, because wave heights are also dependent on the track location with respect to the island. On top of that, SWAN solves the spectral action balance action by taking into account wave growth by wind, nonlinear transfer of wave energy, bottom friction and wave decay (whitecapping) and breaking. The interactions between the different elements govern the evolution of the shape of the spectrum and thus the wave height. For example, typhoon Pamela (1982), with a maximum wind speed of 48 m/s (category 2), resulted in the model in a wave height of 8.1 m at Ebeye. On the other hand, typhoon Paka (1997) which was characterized by a maximum wind speed of 68 m/s (category

4), resulted in a wave height of only 4.7 m. For storm surges the atmospheric pressure drop is mainly relevant, since wind-driven setup at coral reefs is generally limited.

In the simulations, there is no pattern identified for the peak wave period and the wind speed or wave height. In general, a peak wave period of 9-11 seconds was observed in the model at the peak of the storms. Therefore, we assume a peak wave period of 10 seconds during the peak of the modeled storms in XBeach. In reality, it is possible that the peak in wave height will not occur simultaneously with the peak in storm surge level. In order, to evaluate the impact of a worst-case scenario we will assume that those effects will occur exactly at the same time.

The results of Figure 9 are used as input to carry out an EVA and to determine the wave height and storm surge levels for different return periods at Ebeye. The result of the EVA is shown in Table 2, in particular the maximum wave height and storm surge for five return periods (RP = 5, 10, 30, 50 and 100 years) for the current and future scenarios. An 11% increase in wind speed and pressure drop will result on average in 8% larger wave height and 6% increase in surge. Moreover, future extreme values will get proportionally larger for higher return periods, meaning that the most destructive events will lead to even more catastrophic consequences.

Table 2 Maximum significant wave height (Hs) and storm surges (SSL) for Ebeye as a result of typhoons for the current scenario and the future scenario based on an EVA of 47 typhoons for 5 return periods (5, 10, 30, 50 and 100 years).

	Maximum Hs (m)		**Maximum SSL (m)**	
Return period [years]	**current**	**2100**	**current**	**2100**
5	4.8	5.1	0.10	0.10
10	5.9	6.3	0.14	0.14
30	7.2	7.8	0.19	0.20
50	7.7	8.3	0.22	0.24
100	8.2	9.0	0.26	0.30

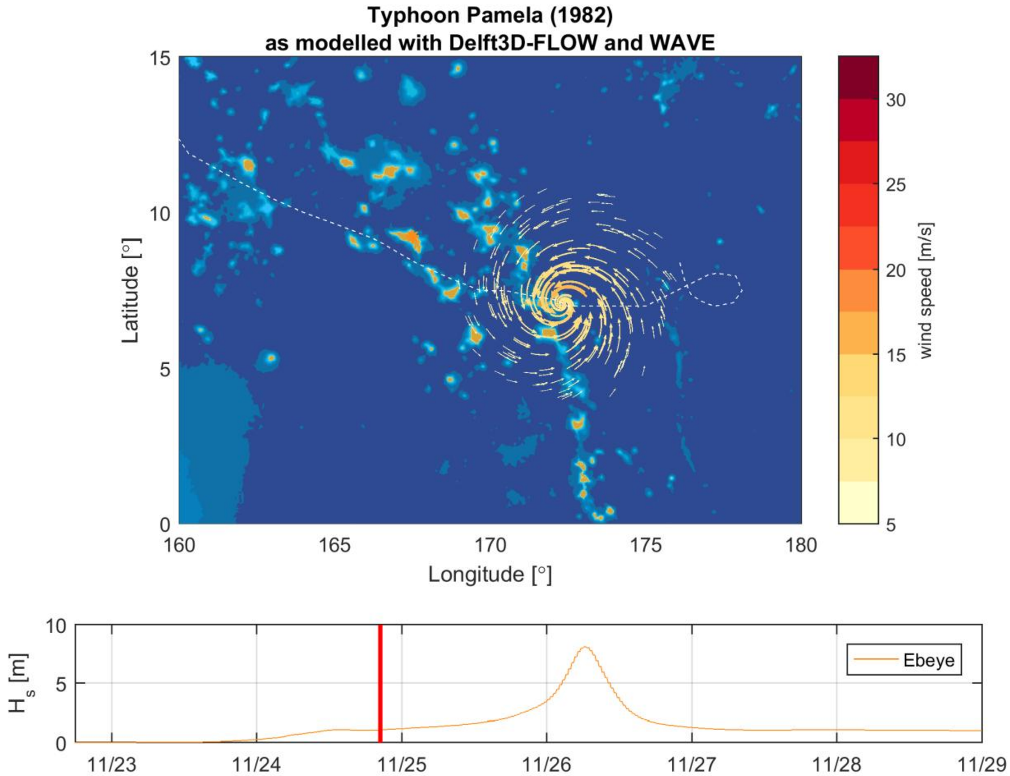

Figure 7 Snapshot of the modeled wind speeds during typhoon Pamela (1982) including the resulting wave height at two atolls.

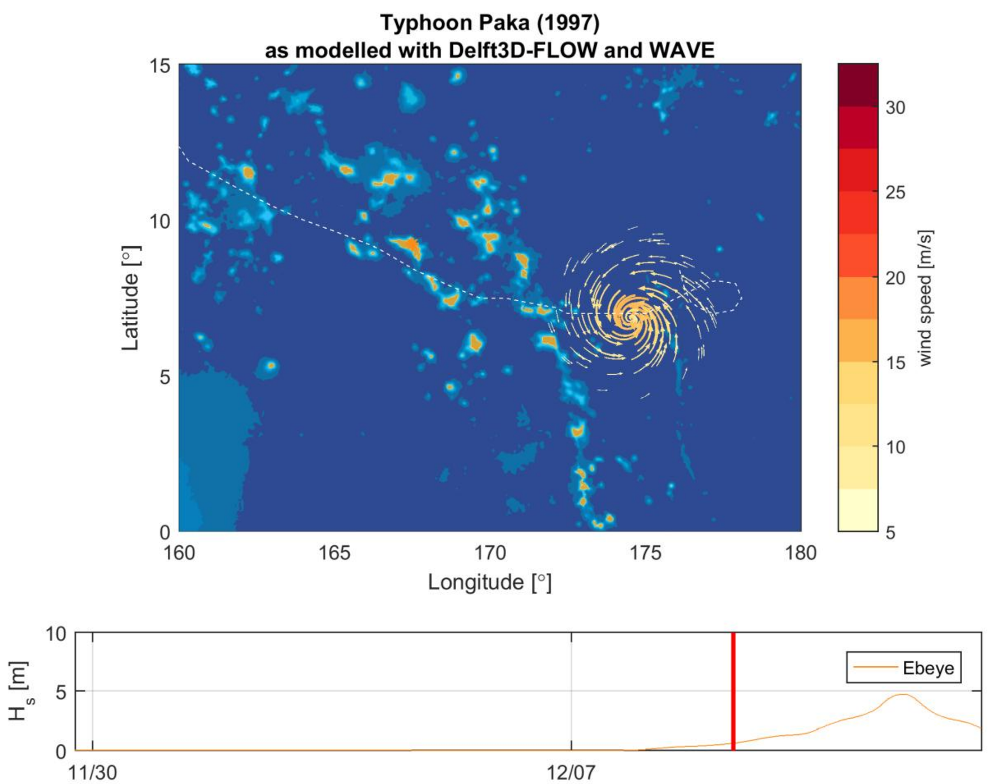

Figure 8 Snapshot of the modeled wind speeds during typhoon Paka (1997) including the resulting wave height at two atolls.

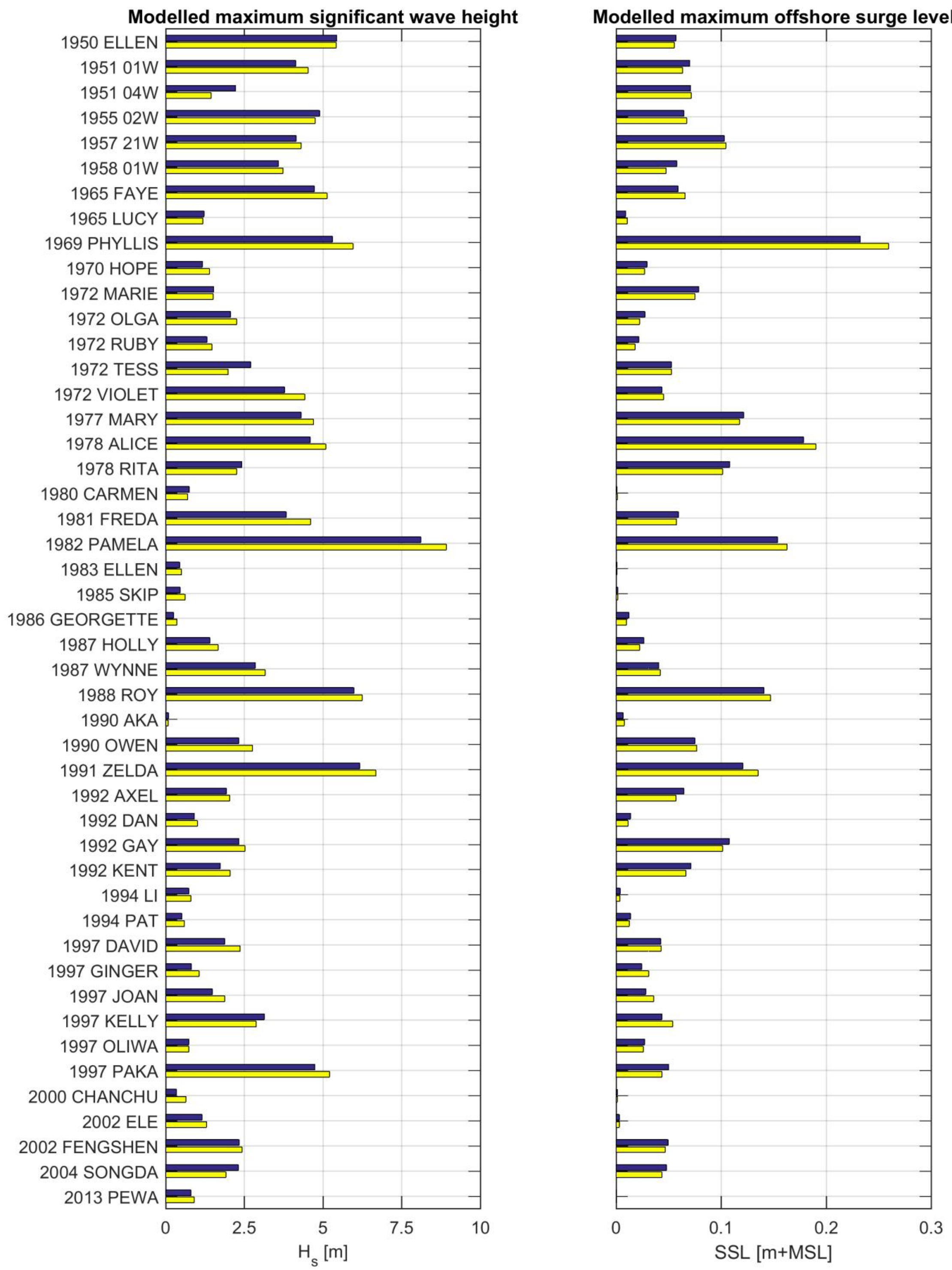

Figure 9   Maximum modeled significant wave height and surge at Ebeye for each simulated typhoon event for the current situation (blue) and the future situation of 2100 (yellow)

Nearshore impact: atoll flooding

The flooding caused by typhoon waves with a 30 year return period (H_s = 7.2 m) is shown as an example to illustrate which parts of the islands are mostly affected in the present situation (Figure 10). The impact of typhoon waves with other return periods is expressed as percent of flooded island area. This percentage depends on the definition of flooding and is thus given for both a minimum flooding depth of 20 cm and a minimum flooding depth of 50 cm (Table 3). Moreover, the Expected Annual Affected People (EAAP; Giardino et al., in preparation) is used to quantify social risk. The EAAP is calculated by integrating the average number of people affected by a water depth of 20 cm or more over the frequency.

As may be expected, the lower parts of the island are the most affected. These are located in the northern part of Ebeye and closer to the lagoon. Higher parts of the island or areas safeguarded by seawalls are more protected.

Generally, the flooding area during typhoon conditions with return periods of 1/5 and 1/10 years is fairly small (respectively 8% and 9%, assuming a threshold for flooding depth of 50 cm; see Table 3). For larger return periods, the offshore wave height and surge increases and results in very rapid large atoll flooding. This is because larger offshore waves will lead to an increase in the wave-induced setup on the reef and higher infragravity waves, both resulting in more flooding. The EAAP due to typhoons in the current situation is estimated to be 750 (6% of the entire population).

Table 3 Percentage of island flooding induced by typhoon waves with return periods 5, 10, 30, 50 and 100 years. The % relative to the island area is given for a minimum flooding depth of 20 cm and 50 cm. Color coded with 0-33% green, 34-66% orange and 67-100% red.

RP [yr]	**Hs [m]**	**[%] of island flooding**	
		Flooding depth > 20 cm	**Flooding depth > 50 cm**
5	4.8	13%	8%
10	5.9	20%	9%
30	7.2	60%	28%
50	7.7	81%	54%
100	8.2	92%	78%

In Table 4, results from different simulations have been presented in order to show the relative impact of changes in sea level and typhoon intensity on the flooded area. For time horizons 2100 under RCP 8.5 and more intense typhoons the flooding extent increases. This is illustrated for a return period of 1/30 years by 2100 in Figure 11. The increase in the amount of flooding for relatively frequent events (return period 1/5, 1/10 and 1/30 years) by 2100 is especially worrying. For example, an event with a return period of 1/10 years will lead to an increase in flooded area from 9% in the current situation to 53% by 2100 (increase of a factor 5), see Table 4. Moreover, The EAAP increases from 750 to 4,701 (increase of 526%).

The effect of intensified typhoons is higher offshore wave heights and therefore more atoll flooding via a larger wave setup on the reef and more infragravity generation. This effect is especially visible for lower wave heights and return periods. For higher return periods (50-100 years) under a sea level rise of 0.78 m almost the entire atoll will already be fully flooded even without any change in the magnitude of the expected typhoons. Stronger typhoon winds result in an increase of the EAAP from 750 to 971 (increase of 29%).

The effect of sea level rise is higher extreme water levels at the coastline, but relatively speaking, less wave setup and infragravity waves due to higher tidal water level on the reef. This effect is visible for all modeled return periods, but is stronger for relatively frequent events (return period 1/5, 1/10 and 1/30 years). With only sea level rise the EAAP increases from 750 to 4,158 (increase of 454%).

Combing these results, one can estimate that the stronger typhoons at Ebeye are responsible for only 5% of the increase in EAAP and the sea level rise for 82%. The remaining 13% are related to feedback loops between higher offshore waves, higher water levels on the reefs and wave heights on the reefs. The reason for this relatively low influence in atoll flooding as a result of intensification of typhoons is related to the hydrodynamic processes in coral reef environments which are inherently different compared to coastlines with a wide continental shelf. The majority of higher offshore waves break at the fore reef and only part of the energy results in more flooding (wave-induced setup and infragravity generation).

Table 4 Percentage of island flooding induced by typhoon waves with return periods 5, 10, 30, 50 and 100 years. The % relative to the island area is given for a minimum flooding depth of 50 cm. Colour coded with 0-33% green, 34-66% orange and 67-100% red.

	[%] of island flooding			
RP [yr]	**Typhoon= +0% SLR = 0 m**	**Typhoon= +11% SLR = 0.78 m**	**Typhoon= +0% SLR = 0.78 m**	**Typhoon= +11% SLR= 0 m**
5	8%	35%	31%	8%
10	9%	53%	43%	10%
30	28%	93%	76%	62%
50	54%	99%	91%	76%
100	78%	100%	98%	88%
EAAP	750	4.701	4,158	971

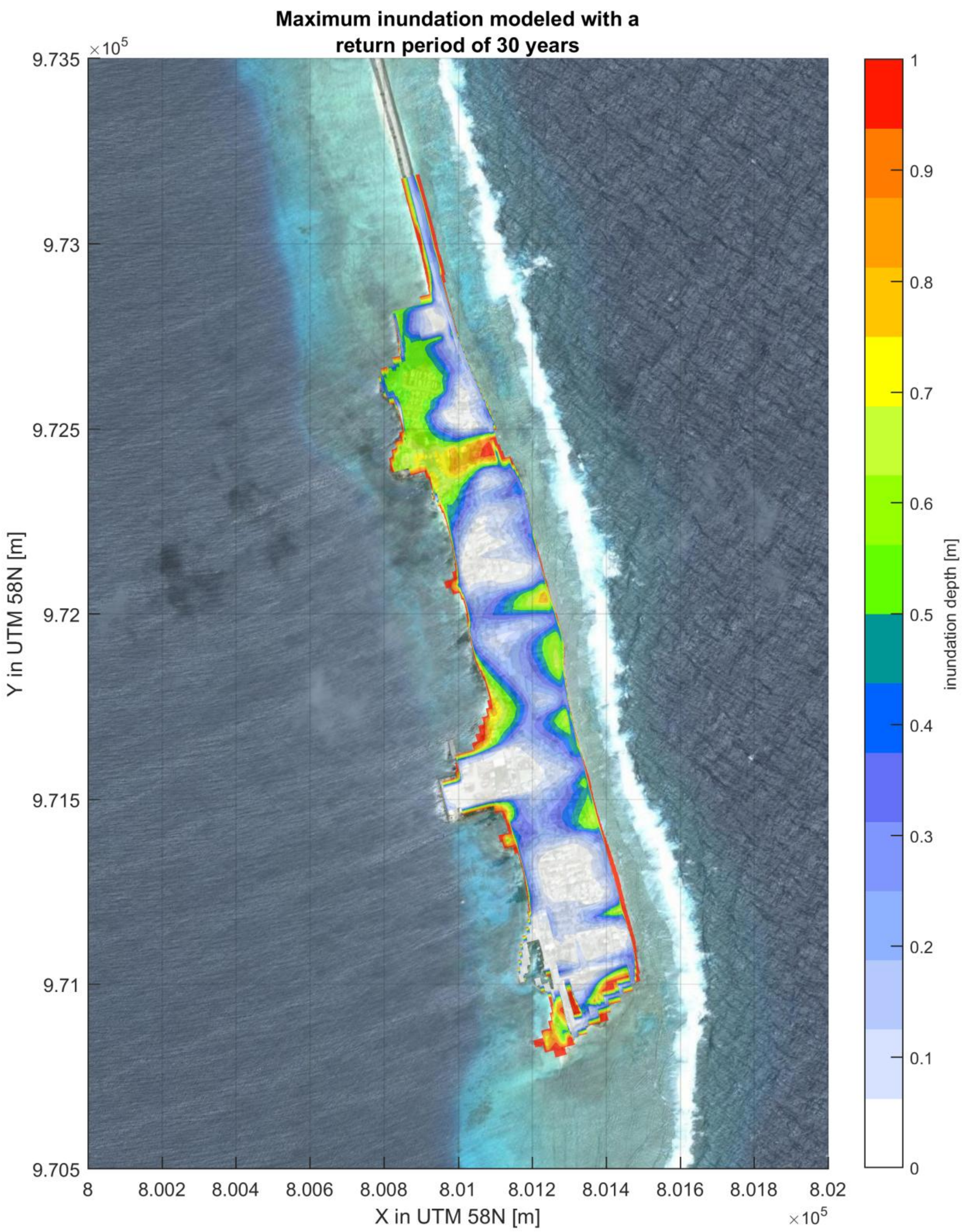

Figure 10 Flooding map showing the impact of typhoon waves for the current situation with an offshore wave height of Hs = 7.2 m (return period of 30 years).

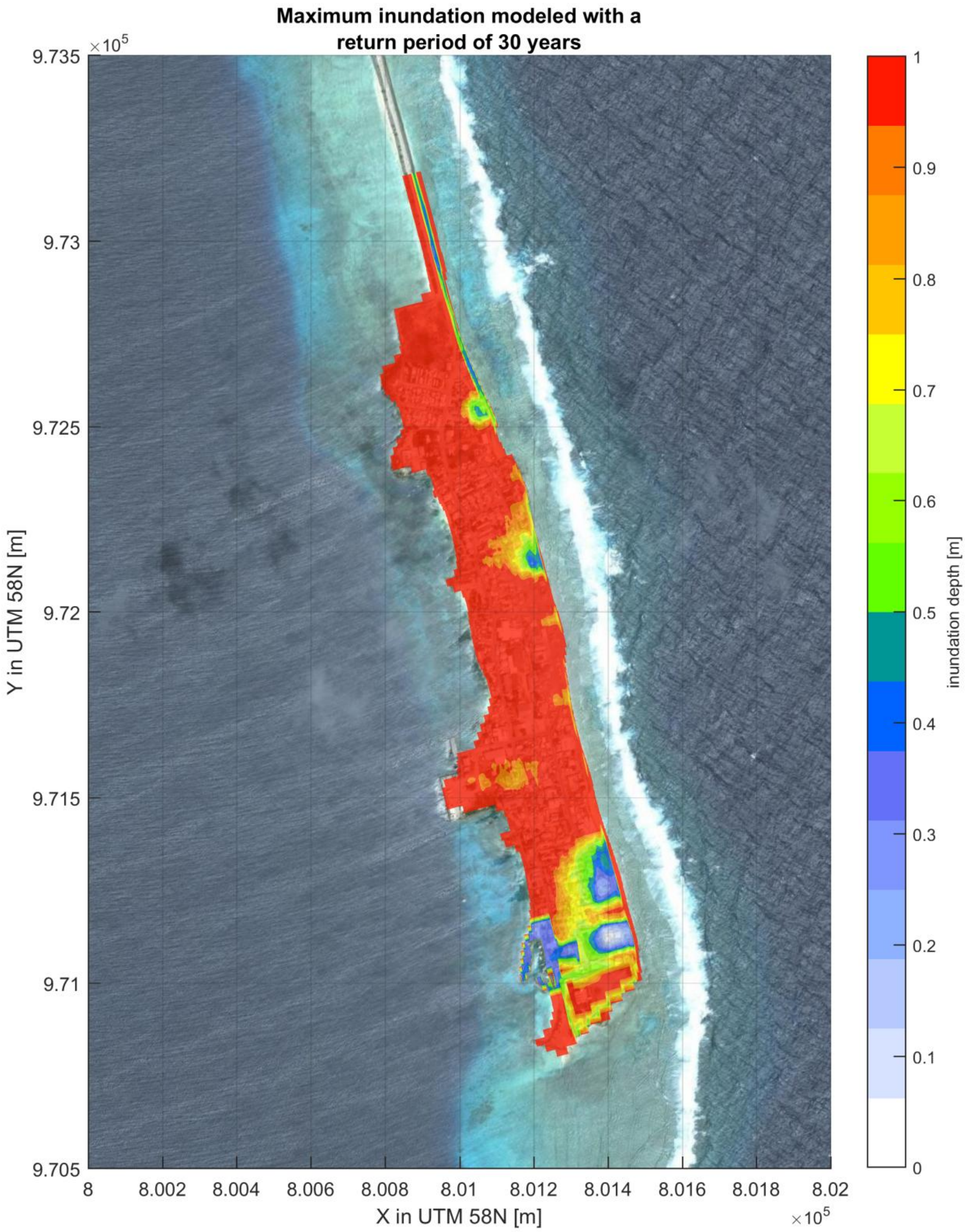

Figure 11 Flooding map showing the impact of typhoon waves for the 2100 situation, including sea level rise and intensified typhoons and resulting in an offshore wave height of Hs = 7.8 m (return period of 30 years).

5. **Discussion**

The results from the numerical modeling study presented in this paper have quantified the impacts of coastal hazards due to typhoons at Ebeye. Unfortunately, no measurements were available at the island and therefore a validation of the model at this location was not possible. However, the methodology has been validated by Nederhoff et al. (in preparation) at the South Pacific specifically for Cyclone Debbie (2017). Moreover, the model performances of the XBeach model have been verified by Giardino et al. (2016) by comparing the calculated wave heights and water levels on the reef with measured values during a large swell event that occurred in March 2014 at Roi-Namur, located at the northern tip of Kwajalein Atoll (Quataert et al., 2015). The results presented in this paper should therefore be interpreted as relative changes (i.e. to assess the effect of climate change) rather than as absolute values.

Detailed bathymetric and topographic data is essential for carrying out an accurate impact assessment at atolls due to their low-lying topography. Unfortunately, field data for this study were rather limited. Therefore, for follow-up studies it would be highly advisable to collect more detailed data (e.g. topographic and bathymetry surveys, wave height measurements, etc.).

6. **Conclusions**

Based on an extreme value analysis for 47 individual typhoons, offshore wave heights at Ebeye were estimated between 4.8-8.2 m, and surge levels between 0.10-0.26 m, for corresponding return periods ranging between 5 and 100 years. As a result of climate change, typhoon wind speeds may increase resulting in 6-8% higher waves and storm surge levels.

Typhoons with higher sustained wind speeds do not necessarily result in higher wave heights. The computed wave height and storm surges are strongly dependent on the exact track location with respect to the island and non-linear wind-wave interactions. Moreover, for storm surges, the atmospheric pressure drop is the most relevant parameter since wind-driven setup at coral reefs is generally limited.

For large return periods (30, 50 and 100 years), large-scale impacts of typhoons on Ebeye are expected. For lower return periods (5 and 10 years) limited impact is expected (<10% atoll flooding). As a result of sea level rise and intensification of typhoons due to climate change, the impact at Ebeye potentially increases by more than 500% until 2100. Stronger typhoons are responsible for 5% of the observed increase in impact, 82% is related to sea level rise and the remaining 13% is related to non-linear interactions on the reef between the two.

This paper shows that it is important to quantify impacts of coastal hazards in an objective manner with process-based models like Delft3D and XBeach. Coastal engineering experiences on dissipative beaches cannot be applied one-on-one with coral reef environments. Moreover, the effects of availability heuristic on low-frequency events, especially in combination with climate change, can result in cognitive biases of people. In this case study, the more slowly-moving but statistically plausible sea level rise is proven to be much more significant in terms of atoll flooding than the statistically less certain typhoon intensification.

7. **Acknowledgements**

The project was financed by the World Bank, and frames within the Small Island State Resilient Initiative (SISRI) implemented by the GFDRR (The World Bank).

8. **References**

Booij, N., Ris, R. C., & Holthuijsen, L. H. (1999). A third-generation wave model for coastal regions. I- Model description and validation. *Journal of Geophysical Research*, *104*, 7649–7666. http://doi.org/10.1029/98jc02622

Church, J. A., & Roemmich, D. (2010). Ocean temperature and salinity contributions to global and regional sea-level change. *Understanding Sea-Level Rise and Variability*, 143–176. http://doi.org/10.1002/9781444323276.ch6

Egbert, G. D., & Erofeeva, S. Y. (2002). Efficient inverse modeling of barotropic ocean tides. *Journal of Atmospheric and Oceanic Technology*, *19*(2), 183–204. http://doi.org/10.1175/1520-0426(2002)019<0183:EIMOBO>2.0.CO;2

Ferrario, F., Beck, M. W., Storlazzi, C. D., Micheli, F., Shepard, C. C., & Airoldi, L. (2014). The effectiveness of coral reefs for coastal hazard risk reduction and adaptation. *Nature Communications*, *5*(May), 3794. http://doi.org/10.1038/ncomms4794

Fujita, T. (1952). Pressure Distribution within Typhoon. *Geophysical Magazine*.

Gerritsen, F. (1980). Wave attenuation and wave set-up on a coastal reef. In *Proc.17th Int. Conf. Coastal Eng* (pp. 444–461).

Giardino, A., Nederhoff, C. M. & Vousdoukas, M. I. (in preparation). A Methodology for multi-hazard and risk assessments for small islands in view of climate change. Case study: Ebeye Island. *Planned to be submitted to Journal Regional Environmental Change*.

Giardino, A., Nederhoff, C. M., Gawehn, M., Quataert, E., & Capel, A. (2016). *Coastal Risk Assessment for Ebeye*. Washington, DC.

Gross, J. M., Demaria, M., Knaff, J. A., & Sampson, C. R. (2004). A new method for determining tropical cyclone wind forecast probabilities, *570*(2), 2–4.

Hasegawa, A., & Emori, S. (2005). Tropical Cyclones and Associated Precipitation over the Western North Pacific: T106 Atmospheric GCM Simulation for Present-day and Doubled CO2 Climates. *Sola*, *1*, 145–148. http://doi.org/10.2151/sola.2005-038

Holland, G. ., Belanger, J. ., & Fritz, A. (2010). A Revised Model for Radial Profiles of Hurricane Winds. *American Meteorological Society*, 4393–4401. http://doi.org/10.1175/2010MWR3317.1

IPCC. (2013). *Climate Change 2013 - The Physical Science Basis. Intergovernmental Panel on Climate Change*. http://doi.org/10.1038/446727a

Kleptsova, O., Pietrzak, J. D., & Stelling, G. S. (2009). On the accurate and stable reconstruction of tangential velocities in C-grid ocean models. *Ocean Modelling*, *28*(1–3), 118–126. http://doi.org/10.1016/j.ocemod.2008.12.007

Knutson, T. R., McBride, J. L., Chan, J., Emanuel, K. A., Holland, G., Landsea, C., … Sugi, M. (2010). Tropical cyclones and climate change. *Nature Geoscience*, *3*(3), 157–163. http://doi.org/10.1038/ngeo779

Lesser, G. R., Roelvink, J. A., van Kester, J. a. T. M., & Stelling, G. S. (2004). Development and validation of a three-dimensional morphological model. *Coastal Engineering*, *51*(8–9), 883–915. http://doi.org/10.1016/j.coastaleng.2004.07.014

Nederhoff, C. M., Van Ormondt, M., & Giardino, A. (in preparation). Estimates of tropical cyclone size parameters based on best track data. *Planned to be submitted to Monthly Weather Review.*

Owen, S. D., Kench, P. S., & Ford, M. (2016). Improving understanding of the spatial dimensions of biophysical change in atoll island countries and implications for island communities: A Marshall Islands' case study. *Journal of Applied Geography*.

Pomeroy, A., Lowe, R., Symonds, G., Van Dongeren, A., & Moore, C. (2012). The dynamics of infragravity wave transformation over a fringing reef. *Journal of Geophysical Research: Oceans*, *117*(11), 1–17. http://doi.org/10.1029/2012JC008310

Quataert, E., Storlazzi, C. S., van Rooijen, A. A., Cheriton, O., & van Dongeren, A. R. (2015). The influence of coral reefs and climate change on wave-driven flooding of tropical coastlines. *Geophysical Research Letters*.

Roelvink, J. A., Reniers, A. J. H. M., van Dongeren, A. R., van Thiel de Vries, J. S. M., McCall, R. T., & Lescinski, J. (2009). Modelling storm impacts on beaches, dunes and barrier islands. *Coastal Engineering*, *56*(11–12), 1133–1152. http://doi.org/10.1016/j.coastaleng.2009.08.006

Schwerdt, R. W., Ho, F. ., & Watkins, R. R. (1979). Meteorological criteria for standard project hurricane and probable maximum hurricane windfields, gulf and east coasts of the United States NOAA Technical Report NWS 23, (September).

Symonds, G., Huntley, D. A., & Bowen, A. J. (1982). Long wave generation by a time-varying breakpoint. *Journal of Geophysical Research*, 492–498. http://doi.org/10.1029/JC087iC01p00492

Vetter, O., Becker, J. M., Merrifield, M. A., Pequignet, A. C., Aucan, J., Boc, S. J., & Pollock, C. E. (2010). Wave setup over a Pacific Island fringing reef. *Journal of Geophysical Research: Oceans*, *115*(12), 1–13. http://doi.org/10.1029/2010JC006455

Vickery, P. J., & Wadhera, D. (2008). Winds of Hurricanes from Flight-Level Pressure and H * Wind Data. *Journal of Applied Meteorology and Climatology*. http://doi.org/10.1175/2008JAMC1837.1

Wright, T. (2004). Tropical storm atlas formation and impacts at Kwajalein atoll, 1–10.

9. **Appendixes**

Table 5 Storm conditions considered in this study showing the typhoon names, year of occurrence, maximum sustained winds and minimal pressures with a minimal intensity of a tropical storm (T.S.) sorted per year

Typhoon name	Year	Maximum sustained wind (m/s)	Minimal atmospheric pressure (mbar)	Category
ELLEN	1950	33	892	H.1
01W	1951	64	870	H.4.
04W	1951	40	886	H.1
02W	1955	48	888	H.2.
21W	1957	62	865	H.4.
01W	1958	78	847	H.5.
SUSAN	1963	76	842	H.5.
ELLEN	1964	25	900	T.S.
LUCY	1965	82	851	H.5.
FAYE	1965	77	836	H.5.
MARIE	1966	56	854	H.3.
PHYLLIS	1969	46	873	H.2.
HOPE	1970	81	810	H.5.
TESS	1972	71	846	H.5.
MARIE	1972	60	843	H.4.
OLGA	1972	60	846	H.4.
RUBY	1972	59	849	H.4.
VIOLET	1972	30	897	T.S.
MARY	1977	52	851	H.3.
RITA	1978	82	792	H.5.
ALICE	1978	59	837	H.4.
06P	1979	41	869	H.1
CARMEN	1980	32	887	T.S.
FREDA	1981	54	851	H.3.
PAMELA	1982	54	847	H.3.
ELLEN	1983	66	837	H.4.
SKIP	1985	42	874	H.1
GEORGETTE	1986	36	874	H.1
WYNNE	1987	68	829	H.4.
HOLLY	1987	74	812	H.5.
ROY	1988	57	847	H.3.
AKA	1990	30	895	T.S.
OWEN	1990	63	838	H.4.
ZELDA	1991	38	877	H.1
AXEL	1992	33	883	H.1
KENT	1992	59	844	H.4.
ZACK	1992	23	894	T.S.
DAN	1992	54	848	H.3.
GAY	1992	67	830	H.4.
LI	1994	37	897	H.1
PAT	1994	44	869	H.2.
PAT	1994	29	883	T.S.
WILDA	1994	55	851	H.3.

ZELDA	1994	67	826	H.4.
KELLY	1997	21	898	T.S.
YULE	1997	37	883	H.1
OLIWA	1997	72	827	H.5.
DAVID	1997	49	854	H.2.
GINGER	1997	62	838	H.4.
JOAN	1997	65	830	H.4.
PAKA	1997	76	839	H.5.
CHANCHU	2000	21	898	T.S.
FENGSHEN	2002	66	825	H.4.
ELE	2002	57	847	H.3.
SONGDA	2004	59	833	H.4.
TALAS	2004	24	893	T.S.
PEWA	2013	35	891	H.1